Bioelectromagnetics 22:79–86 (2001)

Effect of Static Magnetic Field on *E. coli* Cells and Individual Rotations of Ion–Protein Complexes

V.N. Binhi,[1]* Ye. D. Alipov,[2] and I. Ya. Belyaev[2,3]

[1]*General Physics Institute Russian Academy of Sciences, Moscow, Russia*
[2]*Moscow Engineering Physics Institute, Moscow, Russia*
[3]*Department of Molecular Genome Research, Stockholm University, Stockholm, Sweden*

The effect of week static magnetic fields on *Escherichia coli* K12 AB1157 cells was studied by the method of anomalous viscosity time dependencies (AVTD). The AVTD changes were found when *E. coli* cells were exposed to static fields within the range from 0 to 110 μT. The dependence of the effect on the magnetic flux density had several extrema. These results were compared with theoretical predictions of the ion interference mechanism. This mechanism links the dissociation probability of ion–protein complexes to parameters of magnetic fields. The mechanism was extended to the case of rotating complexes. Calculations were made for several ions of biological relevance. The results of simulations for Ca^{2+}, Mg^{2+}, and Zn^{2+} showed a remarkable consistency with experimental data. An important condition for this consistency was that all complexes rotate with the same speed ∼18 revolutions per second (rps). This suggests that the rotation of the same carrier for all ion–protein complexes may be involved in the mechanism of response to the magnetic field. We believe that this carrier is DNA. Bioelectromagnetics 22:79–86, 2001.

Key words: metalloprotein; ion binding; genome; viscosity; ion interference; quantum mechanisms

INTRODUCTION

An increasing number of investigations have shown that nonthermal alternating (AC) magnetic fields (MFs) of extremely low frequency (ELF) affect biological systems [Frey, 1994; Goodman et al., 1995]. The effects of AC fields have been observed within relatively narrow frequency bands at so-called resonance frequencies [Liboff, 1985; McLeod et al., 1987; Blackman et al., 1994; Fitzsimmons et al., 1994; Prato et al., 1995; Alipov and Belyaev, 1996]. Relatively narrow windows were also observed in the amplitude dependencies of the AC field effects [Liboff et al., 1987; Blackman et al., 1994; Prato et al., 1995]. It has been found [Liboff, 1985; Blackman et al., 1985] that the local static MF can significantly influence the effects of AC fields. The static MF is currently considered as an important parameter during exposure to AC fields [Blanchard and Blackman, 1994; Belyaev et al., 1994; Prato et al., 1995].

In several papers, the resonance-like effects were discussed with respect to the cyclotron frequencies Ω_c for some ions of biological relevance such as calcium, magnesium and others [Liboff, 1985; Liboff et al., 1987; McLeod et al., 1987]. Several mechanisms were suggested for the observed effects of AC fields. The mechanism of ion cyclotron resonance [Liboff et al., 1987] predicted effects at cyclotron frequencies and their harmonics, while the mechanism of parametric resonance [Lednev, 1991; Blanchard and Blackman, 1994] dealt with cyclotron frequencies and their subharmonics. Frequency windows were shifted directly with static magnetic field (DC). Liboff explained this fact based on proportionality between DC field and the cyclotron frequency for an ion with charge q and mass M, $\Omega_c = qB_{DC}/M$ [Liboff, 1985].

Contract grant sponsor: Swedish Council for Work Life Research; Swedish Electrical Utilities Research and Development Company; Swedish Radiation Protection Institute.

*Correspondence to: Dr. V. N. Binhi, General Physics Institute RAS, 38, Vavilova St., Moscow 117942, Russian Federation. E-mail: binhi@dataforce.net, Internet: http://www.dataforce.net/~binhi

Received 3 August 1998; Final revision received 6 March 2000

It has been previously found [Belyaev et al., 1994] that static MFs can affect *Escherichia coli* cells, resulting in the same changes in chromatin conformation as was observed after exposure of cells to combined AC/DC fields. The dependence of this effect on magnetic induction had several extrema. Cyclotron and parametric resonance mechanisms could not explain the observed dependence because of the absence of the AC field, which could resonate with characteristic frequencies like Ω_c of ionic oscillators. The first theoretical study in terms of the same classical mechanism for both DC and AC/DC bioeffects was based on phase modulation of natural intracellular oscillations by magnetic fields [Belyaev et al., 1994]. This study predicted the wave-like dependence of the DC field effects on magnetic flux density, but the effective windows for the magnetic flux density were not calculated.

Consideration of ion dynamics in viscous media and in heat bath was undertaken by Moggia et al. [Moggia et al., 1997]. Bioeffects of MF have been associated by Chiabrera and colleagues [Chiabrera et al., 1991] with quantum transitions of ions which are bound to proteins in anhydrous cavities. In general, this approach could be equally applied to the effects of both static and alternating MFs. However, no predictive formulas were derived in these works.

Recently, a new quantum-mechanical mechanism was suggested. This mechanism is based on an interference of quantum states of ions bound to protein inside an idealized cavity [Binhi, 1997a]. According to this mechanism, superposition of the ion states forms a nonuniform pattern of probability density of the ion. This pattern consists of a row of more and less dense segments. In a DC field, the pattern rotates in the cavity with the cyclotron frequency. Exposure to the AC field of specific parameters retards the rotation for the large part of a rotation cycle and facilitates escape of ion from the cavity. This escape may influence equilibrium of biochemical reactions to result in a biological endpoint. The predictions of the ion interference mechanism were in good agreement with some effects of combined DC/AC MFs [Binhi, 1997b] and pulsed MFs [Binhi, 1998]. In the absence of AC field, the mechanism predicted only one extreme for dependence of biological effect on DC magnetic induction. This extreme should be observed at ''zero'' static MF. On the other hand, the experiments with *E. coli* cells revealed several extrema in such magnetic conditions [Belyaev et al., 1994]. We noticed that these additional extrema might be explained assuming that ion–protein targets of DC fields could naturally rotate inside cells. Indeed, such rotations normally occur in biological systems.

MOLECULAR ROTATIONS IN *E. coli* CELLS

Classical example of rotation in *E. coli* is a rotary flagellar motor. In *E. coli*, several filaments come together to form a bundle that rotates at a speed around 300 revolutions/sec (rps) and drives the cell body forward at speeds of a few tens of microns per second. The cell body counter-rotates at several rps [Lowe et al., 1987]. The rotation of filaments at speeds within the ELF range was well characterized in *E. coli* cells [Berry and Berg, 1996]. The rotation of ATPase that is embedded in the membranes of mitochondria, chloroplasts, and bacteria has been recently characterized [Noji et al., 1997]. Stable rotation of the F_1-ATPase with an attached fluorescent actin filament was observed in vitro in the presence of Mg^{2+}-ATP. The speed of rotation depended on the length of the attached filament, was at most 4 rps, but should be higher without a filament. The Vaccinia type I topoisomerase follows a free rotation mechanism for removing supercoils from DNA, and the rotation rate of the cleaved DNA strand is about 20 rps [Stivers et al., 1997].

The process of transcription is connected with relative rotation of DNA and RNA polymerase [Cook et al., 1992] and may result in periodic rotation of RNA polymerase around DNA. Metal ions can be included in proteins of the transcription complex, such as transcription factors and RNA polymerase. For example, *E. coli* RNA polymerase contains two Zn^{2+} ions per molecule of enzyme, one ion in both the substrate binding subunit β and the DNA template binding subunit β' [Miller et al., 1979]. Three Mg^{2+} ions are required for the formation of a transcription active complex [Suh et al., 1992]. The β' subunit of *E. coli* RNA polymerase contains the preserved motif with three asparates and is assumed to participate in formation of the binding pocket of Mg^{2+} [Zaychikov et al., 1996]. An exchange of Zn ions induced a conformational switch in transcription factors, which could have a significant effect on transcription activation [Gardner et al., 1991].

Other divalent ions may substitute for Zn^{2+} ion in *E. coli* RNA polymerase and transcription factors [Panth et al., 1991; Gardner et al., 1991]. Transcription factors with zinc-finger motif were well-characterized in different types of cells including prokaryotes [Pountney et al., 1997]. Therefore, there are several examples of the macromolecular rotations in *E. coli* cells covering the range of 4–300 rps. These data about rotations of ion–protein complexes allowed us to consider possible effects of static MFs on ion–protein complexes at such rotations using the ion interference mechanism.

In the present work, we i) extend the ion interference mechanism [Binhi, 1997a,b,c] to the case of rotating ion–protein complexes, ii) continue the investigation of the effect of static MFs on conformation of DNA–protein complexes such as nucleoids in *E. coli* cells [Belyaev et al., 1994], and iii) compare the experimental results with theoretical predictions based on the ion interference. The rationale for this comparison is the well-known fact that the conformation of nucleoids and chromatin are strongly dependent on the concentration of different ions. For example, Na ions resulted in relaxation of chromatin and Mg ions resulted in condensation of chromatin from V-79 cells [Heussen et al., 1987]. The changes in chromatin conformation were observed under exposure of *E. coli* cells to static MF and ELF MFs and after incubation of cells in media with different concentrations of Mg and Na ions [Belyaev et al., 1994; Alipov and Belyaev, 1996; Ushakov and Belyaev, unpublished data]. In addition, the ELF MF effects were inhibited by the specific chelator of Ca ions, EGTA [Belyaev et al., 1999]. Therefore, several different ions may be involved in control of chromatin conformation, both in intact and magnetically exposed cells.

THEORETICAL MODEL

For most ions of biological relevance, even at $T = 300$ K, the de Broglie wavelengths are three to six times less than their radii, that is, close to the binding cavity size. For example, the ion–ligand distance in the calcium-specific site in troponin C is 2.4 Å [Satyshur et al., 1988]. This site also binds magnesium. Bonding radii of Ca^{2+} and Mg^{2+} are 1.74 Å and 1.36 Å, respectively. The de Broglie wavelengths, $\lambda = 2\pi\hbar/p$, of calcium and magnesium are 0.28 Å and 0.36 Å at the mean thermal momentum $p = \sqrt{2MkT}$. Thus, at the atomic scale, ions display quantum properties that cannot be reduced to the behavior of classical particles. Quantum mechanics appears therefore to be necessary to describe the ion states within the cavity.

The ions bound to proteins within the cavities will be regarded using a quantum-mechanical approach described previously [Binhi, 1997a]. Briefly, the Hamiltonian operator of the Schrodinger equation for an ion with charge q and mass M in a central potential U is

$$\mathcal{H} = \frac{\mathbf{P}^2}{2M} + U - \frac{q\hbar}{2M}\mathbf{LB}. \qquad (1)$$

Here $\mathbf{P} = -i\hbar\nabla$ is momentum operator and $\mathbf{L} = i\mathbf{r} \times \nabla$ is angular momentum operator. The origin of spherical coordinates is placed in the center of the potential U. An ion enters or escapes from the cavity at a point which is called ionic gate. The MF can affect this process, resulting in a biological effect. Given the magnetic flux density $B_{\mathrm{DC}} + B_{\mathrm{AC}}\cos(\Omega t)$ in parallel with z-axis, the probability density of an ion near the ionic gate with angular position $\varphi = \varphi_0$, is

$$p(\varphi_0, t) = \sum_{mm'} a_{mm'} \exp\left[i\Delta m\left(\varphi_0 + \omega_0 t + \frac{\omega_1}{\Omega}\sin(\Omega t)\right)\right], \qquad (2)$$

where $\omega_0 = qB_{\mathrm{DC}}/2M$, $\omega_1 = qB_{\mathrm{AC}}/2M$, $\Delta m = m' - m$, $m = 0, \pm 1, \ldots$ is the magnetic quantum number. The matrix elements $a_{mm'}$ are constants which determine the initial conditions for the ion entering the cavity at $t = 0$. For example, a_{mm} is an initial population of the state with the magnetic quantum number m.

In general, the probability of escape P depends nonlinearly on the ionic density Eq. 2. The dependence can be reduced to a polynomial series near the permanent component $\bar{p}$ of p. Two initial terms, linear and quadratic, of the expansion $P(p) = P(\bar{p}) + P'_p\tilde{p} + P''_{pp}\tilde{p}^2/2 + \ldots$, where $\tilde{p} = p - \bar{p}$, are left for analysis. Averaging over the time, we get $\overline{P} = c_1 + c_2\overline{\tilde{p}^2}$, where $c_{1,2}$ are constant values. The expression for mean probability of dissociation has several components. The $\overline{\tilde{p}^2}$ term presents a dependence of $\overline{P}$ on the parameters of MF and will be analyzed. In order to simplify calculations, we will neglect relatively fast oscillations of $\tilde{p}$. For this purpose, the smoothing average of $\tilde{p}$ over the mean time T of conformational reaction of the protein is found beforehand. The averaged value of $\tilde{p}(t)$, written as $\tilde{p}_T$, is a $(1/2T)\int_{t-T}^{t+T}\tilde{p}(t')dt'$. The value T may be thought as the characteristic time for the dissociation of ion–protein complex. For example, this time is about 0.05–0.1 *s* for binding of calcium to calmodulin [Forsen and Lindman, 1981]. The final expression for mean "magnetic" component $\mathsf{P} = \overline{\tilde{p}_T^2}$ of P is as follows

$$\mathsf{P} = \sum_{mm'n} |a_{mm'}|^2 \frac{\sin^2 A}{A^2} \mathrm{J}_n^2\left(\frac{\Delta m}{2}\frac{h'}{f'}\right),$$
$$A = \left[\Delta m\frac{\omega_0}{\Omega_c} + nf'\right]\Xi, \qquad (3)$$

where $f' = \Omega/\Omega_{\mathrm{c}}$ and $h' = B_{\mathrm{AC}}/B_{\mathrm{DC}}$ are dimensionless frequency and dimensionless peak value of MF. J_n is the n-th order Bessel function of the first

kind, $\Xi = T\Omega_c$ is the dimensionless parameter of the model.

The rotations of metalloproteins were found in several types of cells. Flagella motor and ATPase have been well-characterized [Berry and Berg, 1996; Noji et al., 1997]. MFs produced by rotating macromolecules, even if they carry relatively large dipole momentum d, may safely be neglected. Their values B_d are much less than the μT level, according to the estimation $B_d \sim \mu_0 d\Omega/4\pi r^2$, where μ_0 is the magnetic permeability of vaccum, r is the distance to dipole.

Let us consider the ions which are bound to the rotating proteins. The position of the ionic gate will be dependent on time. If the macromolecule rotates with angular velocity $\Lambda_k = \Lambda k$ of discrete quantum set $k = 0, \pm 1, \ldots$, the angular coordinate of the gate is

$$\varphi_0 + \Lambda_k t. \tag{4}$$

The ion probability density within rotating protein can be obtained from Eqns. 2 and 4 by substitution of $\omega_0 \to \omega_0 + \Lambda_k$. Therefore, the dissociation probability follows from Eq. 3 after this substitution

$$\begin{aligned} \mathsf{P} &= \sum_{mm'nk} |a_{mm'}|^2 |c_k|^2 \frac{\sin^2 A}{A^2} \mathrm{J}_n^2\left(\frac{\Delta m}{2}\frac{h'}{f'}\right), \\ A &= \left[\Delta m\left(\frac{\omega_0 + \Lambda_k}{\Omega_c}\right) + nf'\right]\Xi, \end{aligned} \tag{5}$$

where $|c_k|^2$ are statistic weights of rotational states. Rotating complexes in the ion interference mechanism were first considered in [Binhi, 1997c]. Detailed calculations for the complexes rotating in both DC and DC-AC MFs at arbitrary angles to the direction of **B**, model validations of the central potential U and the absence of thermal interactions in Eq. 1 are given in [Binhi, 2000].

Providing $B_{AC} = 0$, all Bessel functions except for $\mathrm{J}_0(0) = 1$ disappear in the Eq. 5, resulting in $n = 0$ in the sum Eq. 5. Then the formula for static MF is

$$\mathsf{P} = \sum_{mm'k} |a_{mm'}|^2 |c_k|^2 \frac{\sin^2 A}{A^2}, A = \Delta m\left(\frac{\omega_0 + \Lambda_k}{\Omega_c}\right)\Xi. \tag{6}$$

This formula predicts the maximal effect at $B_{DC} = 0$ (zero MF). Indeed, the P is maximal at $A = 0$, or at $\omega_0 = -\Lambda_k$. It results in

$$(B_{DC})_{max} = -2k\frac{M}{q}\Lambda. \tag{7}$$

For ion–protein complexes which do not rotate ($k = 0$), only the maximum of P is at $B_{DC} = 0$.

Except for the maximum at zero MF, additional extrema might be due to the rotation of ion complexes in accordance with Eq. 7. Therefore, the ion interference mechanism is able to predict a wave-like dependence of effect on magnetic flux density.

MATERIALS AND METHODS

E. coli K12 AB1157 cells grown in 5 ml of Luria broth (trytone "Difco" 10 g/l, yeast extract "Difco" 5 g/l, NaCl 10 g/l) without shaking at 33° C. The cells reached a concentration of about 10^9 cells per milliliter and optical density of OD_{550} =0.92–1.05 for 18 h. This corresponded to early stationary phase of growth [Belyaev et al., 1993]. The cells were centrifuged, 10 min, 2800 g, and diluted in the M9 buffer (3 g/l KH_2PO_4, 0.2 g/l NH_4Cl, 6 g/l Na_2HPO_4, 1 g/l $MgSO_4$, 0.5 g/l NaCl, pH 7.0) to the concentration of 4×10^7 cell/ml. After dilution, cells were preincubated 30 min before exposure. Preincubation was performed under the same magnetic conditions as cell growth. The ambient horizontal and vertical components of a geomagnetic field were equal to 20 ± 1 μT and 44 ± 1 μT, respectively.

Cells were exposed to DC field by means of two pairs of Helmholtz coils. These coils were designed so that the exposed samples would be in a uniform field. Horizontal static magnetic field was applied by means of a pair of 100 turn, 19.6 cm diameter Helmholtz coils. The coils were oriented in order to create a static field parallel to the horizontal component of the ambient field. Each coil had a resistance of 7.87 Ω and an inductance of 4.77 mH. Vertical field was applied using another pair of 100 turn, 12.8 cm diameter Helmholtz coils. Each coil had a resistance of 5.23 Ω and an inductance of 2.74 mH. The direct current were supplied by two power supplies with stabilization better then 0.025%.

We were concerned about stabilization since some DC power supplies could produce significant ripple currents and AC magnetic fields. The ripple current of the chosen supplies did not produce the oscillating magnetic field more then 30 nT (rms) as measured with 3D ELF field dosimeter. Background ELF magnetic field was 50 nT. At the beginning of experimentation, several experiments were performed using appropriate configuration of static magnetic field created by permanent magnets. In these experiments we obtained the same data as with DC power supplies (not shown). Based on this similarity we assumed that ELF fields induced by ripple currents did not affect the response of cells to the DC field. The experiments with

static magnets were time consuming, and most part of data was obtained with DC power supplies. The static magnetic fields were measured using a magnetometer and calculated by means of measuring a direct current. The measured and calculated values were equal with an accuracy of 1%.

Usually, the cells were exposed in a volume of 3.5 ml during 15 min. The lysis was performed 75 min after exposure, when a maximum effect of magnetic fields on the genome conformation was observed [Belyaev et al., 1994, 1998]. The temperature was measured in exposed samples using microthermocouple with an accuracy of 0.1°C. No measurable heating was observed during incubation of cells in Helmholtz coils. The control cells were concurrently subjected to the same manipulations, except for exposure.

The changes in the genome conformational state were measured using the method of anomalous viscosity time dependencies (AVTD) [Belyaev et al., 1994, 1997]. Application of this method to ELF-exposed *E. coli* cells has been recently described in detail [Balyaev et al., 1998]. Briefly, the AVTD method is based on radial migration of large DNA–protein complexes in the high-gradient hydrodynamic field of a rotary viscometer [Kryuchkov et al., 1995]. Radial migration of molecular complexes toward the rotating rotor causes anomalous changes of viscosity that can be registered by measuring the rotor rotation period as a function of time. This anomalous viscosity time dependence strongly depends on the conformational state of the genome, which in turn is dependent on DNA parameters such as molecular weight, micromedium, and the number of proteins bound to the DNA. The effects of the specific DNA intercalator ethidium bromide on the supercoiling of DNA loops in human lymphocytes have been recently measured with AVTD and neutral comet assay [Belyaev et al., 1999a]. Comet assay has directly confirmed that the increase in AVTD peaks has been caused by relaxation of DNA loops and the AVTD decrease has been caused by chromatin condensation. Both effects were not dealing with DNA breaks, as was shown with the alkaline comet assay.

The AVTDs were measured in the cell lysates at a shear rate of 5.6/s and a shear stress of 0.007 N/m^2. Each AVTD curve is a set of experimental points (period of rotation versus time of measurement) which are recorded by an IBM PC. The maximum period of rotation T corresponds to maximum viscosity and has been previously shown to be the most sensitive AVTD parameter. The significance of differences between mean values in exposed samples $\langle T_{exp} \rangle$ and control samples $\langle T_{con} \rangle$ was evaluated with the Student's t-test in each experiment. Maximum relative viscosity index MRV was used to determine the MF effects:

$$MRV = \langle T_{exp} \rangle / \langle T_{con} \rangle.$$

Results were considered as significantly different at $P < 0.05$. Sham-exposed cells were run under the same conditions as exposed cells. The only difference was disconnection of wires between power supply and Helmholtz coils for sham-exposure. Each version of the experiment included not less than three measurements, which were compared with corresponding variants of intact and sham-exposed cells using the Student's t-test. Comparison of control with sham control revealed no significant differences.

RESULTS AND DISCUSSION

Fifteen independent experiments were conducted. In these experiments, the horizontal magnetic field was compensated to 0 ± 1 μT and the vertical component of static MF field was varied. In each experiment the effect of a 15 min MF exposure was investigated at 8–10 values of magnetic induction. Good reproducibility was observed from experiment to experiment during research that spanned three calendar years. The averaged dependence of the effect on the MF induction is shown in Figure 1. This dependence had several ''windows'' with extrema at the DC field of 0 ± 1, 26 ± 2, 43 ± 2, 61 ± 2, 72 ± 3, 83 ± 3, and 96 ± 3 μT. In each of these windows, 3–7 experimental points around extreme were statistically significantly different from the control level in at least three independent experiments. Within the window at 101–109 μT, the effect was statistically significant in one point, 105 μT. In four windows, 0 ± 1, 43 ± 2, 72 ± 3, and 96 ± 3 μT, magnetic field increased maximum relative viscosity. In other four windows, 26 ± 2, 61 ± 2, 83 ± 3 μT, and 105 ± 3 μT magnetic field resulted in decrease of AVTD. Based on previous investigations, the increase in AVTD corresponds to relaxation of chromatin/DNA loops and, contrary, the decreased AVTD corresponds to condensation of chromatin [Belyev et al., 1999a]. The peak values of the effect decreased from window to window as magnetic flux density increased. The maximum effect was observed at ''zero'' static magnetic field, 0 ± 1 μT. Approximately the same effect was observed in cells which were exposed to zero magnetic field within 20–90 min (not shown).

Calculations were performed for several ions of biological relevance, Li, K, Na, Mg, Ca, Zn, using different values of model parameters. Only one combination of ions, namely magnesium, calcium,

and zinc, led to coincidence of extrema in theoretical and experimental dependencies. Other combinations did not allow to fit all observed extrema. In those cases, the shifts between experimental and theoretical extrema were greater then the width of experimental peak (at a half-height level) at least for one of the peaks. The coincidence appeared to be good provided the same speed of rotation, model parameter Λ, was chosen for all the ion–protein complexes.

The results of calculations, both for each ion and for linear superposition of all ions,

$$\mathrm{P_{sum}} = \mathrm{P_{Ca}} - \mathrm{P_{Mg}} + \mathrm{P_{Zn}} \qquad (8)$$

are presented in the Figure 1 along with experimental data. The small shift between experimental control level $MRV = 1$ and theoretical level $\mathrm{P} = 0$ stems from the fact that the $MRV = 1$ relates to the local geomagnetic field 48 μT. The physical model cannot predict relative amplitudes of peaks. They depend on the subsequent pathways of biochemical signal transduction. For simplicity, the time constant of conformational reaction was $T = 0.1$ s for all ions. This value is characteristic of Ca and Mg-binding proteins as measured with the NMR technique [Forsen and Lindman, 1981]. All ions were considered to rotate with the same angular velocity $\Lambda = 110$/s or 18 rps. Other details of calculation were $|m| < 3$, $|k| < 5$, $a = 1$, $|c_k|^2 = 0.5^{|k|}$. The indicated ranges of m and k provide good approximation to the sum Eq. 6, which converges rapidly over these values. The reduction of c_k reflexes decrease of the statistic weights of rotational states with increase of k.

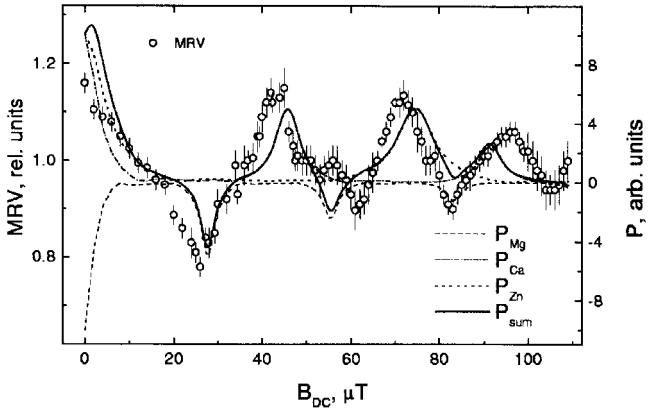

Fig. 1. Comparison of experimental data with results of computer simulations. **Points:** Maximum relative viscosity in cell lysates after exposure *E. coli* cells to static MF. The data of at least three experiments in 4–7 points around each extreme and from 1–3 experiments in other points were averaged based on 15 independent experiments; standard error is shown. **Lines:** The "magnetic" part of dissociation probability for different ions, Ca, Mg, Zn, and linear superposition of these probabilities is shown. The unique combination of these ions provided good coincidence for positions of peaks in experimental and theoretical dependence of the effect on magnetic induction.

Upon choosing the ion species, only the parameter Λ remains to fit the theoretical and experimental positions of peaks in Figure 1. For the best fit, Mg ions act opposite to Ca and Zn ions act in the same direction as Ca. The opposite effects of some ions on conformation of chromatin were described in several papers. For example, ions of Na and Mg resulted in relaxation and condensation of chromatin in V-79 cells, correspondingly [Heussen et al., 1987]. The opposite effects of Na and Mg was observed in our experiments with *E. coli* cells [Ushakov and Belyaev, unpublished data]. It is known that ions of Ca and Mg compete for the binding sites of calmodulin and troponin C [Rainteau et al., 1989]. These proteins change the activity of some enzymes when Ca, not Mg, ions are bound. Therefore, involvement of these ions in the binding process might lead to the opposite biological effects. This is a rationale for summation of the expected effects of Ca and Mg with opposite signs. Contribution of Zn ions to the biological endpoint is assumed to be independent of the Ca and Mg contributions and therefore may also be presented as a part of the sum in Eq. 8.

There is a qualitative agreement between theoretical multipeak curve and experimental data in the Figure 1. The coincidence of calculated and measured positions of the extrema is the consequence of the assumption that natural rotation of ion–protein complexes underlies the effect. According to the model, positions of the peaks depend only on the angular velocity Λ. Other combinations of ions than Ca, Mg, Zn do not provide peaks closer to the experimental peaks as calculated for different Λ. Further investigations may provide a better evidence for the involvement of the specified ions in the observed effects. In particular, only the peaks related to a given ion should be shifted by replacing this ion by its isotope and other peaks should be rather stable.

The ion interference mechanism predicted biological effects of zero field [Binhi, 1997a]. This prediction is supported by experimental data of this paper and previously published results on the sensitivity of *E. coli* cells, human lymphocytes and fibroblasts to zero MF [Belyaev et al., 1994, 1997]. The effect of zero static MF was maximal in this paper. The experiments with static MF allow estimating the effects due to rotating molecules, since the molecules without rotation could react only to zero magnitude of the static MF. Another interesting result is that rotation could be with the same speed for different ions. Based

on these data, we believe that DNA is a suitable carrier for ion–protein complexes rotating with that speed.

The separate sequences of DNA might rotate in respect to attachment sites, transcription, recombination and replication complexes. The process of replication can be excluded because the stationary *E. coli* cells were used in our experiments and cells were kept in M9 buffer before exposure. The speed of elongation during transcription is about 40 nucleotide/s. Transcription is connected with relative rotation of DNA and RNA polymerase [Cook et al., 1992] and may result in periodic rotation of RNA polymerase and several proteins from transcription complexes about the DNA. Providing the period of DNA helix is approximately 10 base pairs, the expected speed of rotation is about 4 rps during transcription.

Enzymes such as topoisomerase I and topoisomerase II may also give rise to rotation of DNA. In particular, the Vacinia topoisomerase I rotates the physiologically cleaved DNA strand with the rate of 20 rps, removing supercoils from DNA [Stivers et al., 1997]. Taking into account the close relationship between transcription and supercoiling, there is no significant contradiction between expected value of 4–20 rps and value calculated above of 18 rps. In our simulations, the reaction time was 0.1 s. Using the obtained frequency of 18 rps, we can calculate that during at least several rotations the system should react with MF. It is likely that the average value of the effect will decrease if the molecules rotate for shorter time. According to the discussed model, the speed 18 rps is the characteristic rate of the ion–protein rotation and presumably is connected to transcription and regulation of DNA topology. To the extent that transcription can proceed with different speeds in cells of different types, the effective values of magnetic intensity can also vary between cell types.

In conclusion, we suggest that transcription and the conformational state of DNA plays an important role in the effect of static MF on *E. coli* cells. It is likely that static MF affects the dissociation probability of Ca, Mg, and Zn ion–protein attached to the same carrier, DNA strands, rotating at a low speed of order of ten rps. Only a qualitative coincidence between experimental and theoretical extrema in MF density dependencies was achieved in this work. More knowledge about the transduction pathways in response to magnetic fields are needed for a better understanding of the weak static MF bioreception.

ACKNOWLEDGMENTS

Authors thank Prof. A. E. Akimov and Prof. M. Harms-Ringdahl for fruitful discussions.

REFERENCES

Alipov YD, Belyaev IY. 1996. Difference in frequency spectrum of extremely-low-frequency effects on the genome conformational state of AB1157 and EMG2 *E. coli* cells. Bioelectromagnetics 17:384–387.

Belyaev IY, Scheglov VS, Alipov YD, Radko SP. 1993. Regularities of separate and combined effects of circularly polarized millimeter waves on *E. coli* cells at different phases of culture growth. Biolectrochem Bioenerget 31:49–63.

Belyaev IY, Matronchik AY, Alipov YD. 1994. The effect of weak static and alternating magnetic fields on the genome conformational state of *E. coli* cells: The evidence for model of phase modulation of high frequency oscillations. In: Allen MJ, editor. Charge and field effects in biosystems—4. Singapore: World Scientific p 174–184.

Belyaev IY, Alipov YD, Harms-Ringdahl M. 1997. Effects of zero magnetic field on the conformation of chromatin in human cells. Biophys Biochem Acta 1336:465–473.

Belyaev IY, Matronchik AY, Alipov YD. 1998. Cell density dependent response of *E. coli* cells to weak ELF magnetic fields. Bioelectromagnetics 19:300–309.

Belyaev IY, Eriksson S, Nygren J, Torudd J, Harms-Ringdahl M. 1999a. Effects of ethidium bromide on DNA loop organisation in human lymphocytes measured by anomalous viscosity time dependence and single cell gel electrophoresis. Biophys Biochem Acta 1428:348–356.

Belyaev IY, Alipov YD, Harms-Ringdahl M. 1999b. Effects of weak ELF on *E. coli* cells and human lymphocytes: role of genetic, physiological and physical parameters, In: F. Bersani, editor. Electricity and magnetism in biology and medicine. NY: Kluwer Academic. 481–484.

Berry RM, Berg HC. 1996. Torque generated by the bacterial flagellar motor close to stall. Biophys J 71:3501–3510.

Binhi VN. 1997a. Interference of ion quantum states within a protein explains weak magnetic field's effect on biosystems. Electro- and Magnetobiology 16:203–214.

Binhi VN. 1997b. The mechanism of magnetosensitive binding of ions by some proteins. Biophysics 42(2):317–322.

Binhi VN. 1997c. Shift of spectral peaks of some magnetobiological effects under rotation of biological sample in ELF magnetic field. The 1997 annual review of research on biological effects of electric and magnetic fields. San Diego, California, November 9–13, BEMS, p 78.

Binhi VN. 1998. Interference mechanism for some biological effects of pulsed magnetic fields. Bioelectrochem Bioenerg 45:73–81.

Binhi VN. 2000. Amplitude and frequency dissociation spectra of ion-protein complexes rotating in magnetic fields. Bioelectromagnetics 21:34–45.

Blackman CF, Benane SG, Rabinowitz JR, House DE, Joines WT. 1985. A role for the magnetic field in the radiation-induced efflux of calcium ions from brain tissue in vitro. Bioelectromagnetics 6:327–337.

Blackman CF, Blanchard JP, Benane SG, House DE. 1994. Empirical test of an ion parametric resonance model for magnetic field interactions with PC-12 cells. Bioelectromagnetics 15:239–260.

Blanchard JP, Blackman CF. 1994. Clarification and application of an ion parametric resonance model for magnetic field interactions with biological systems. Bioelectromagnetics 15:217–238.

Chiabrera A, Bianco B, Caufman JJ, Pilla AA. 1991. Quantum dynamics of ions in molecular crevices under electromag-

netic exposure. In: Brighton CT, Pollack SR, editors. Electromagnetics in medicine and biology. San Francisco: San Francisco Press. p 21–26.

Cook DN, Ma D, Pon NG, Hearst JE. 1992. Dynamics of DNA supercoiling by transcription in *Escherichia coli*. Proc Nat Acad Sci USA 89:10603–10607.

Fitzsimmons RJ, Ryaby JT, Magee FP, Baylink DJ. 1994. Combined magnetic fields increased net calcium flux in bone cells. Calcif Tissue Int 55:376–380.

Forsen S, Lindman B. 1981. Calcium and magnesium NMR in chemistry and biology. Annual Reports on NMR Spectroscopy 11A:183–226.

Frey AH, editor 1994. On the nature of electomagnetic field interactions with biological systems. Austin, Texas: R. G. Landes Co.

Gardner KH, Pan T, Narula S, Rivera E, Coleman JE. 1991. Structure of the binuclear metal-binding site in the GAL4 transcription factor. Biochemistry 30:11292–11302.

Goodman EM, Greenebaum B, Marron MT. 1995. Effects of electromagnetic fields on molecules and cells. Int Rev Cyt 158:279–338.

Heussen C, Nackerdien Z, Smit BJ, Böhm L. 1987. Irradiation damage in chromatin isolated from V-79 Chinese hamster lung fibroblasts. Radiat Res 110:84–94.

Kryuchkov VS, Polunin VA, Alipov YD, Belyaev IY. 1995. Physical model of anomalous viscosity time dependence in solutions of high-polymer DNA-protein complexes. Biofizika 40:1202–1207. In Russian.

Lednev VV. 1991. Possible mechanism for the influence of weak magnetic fields on biological systems. Bioelectromagnetics 12:71–75.

Liboff AR. 1985. Geomagnetic cyclotron resonance in living cells. J Biol Phys 13:99–102.

Liboff AR, Rozek RJ, Sherman ML, McLeod BR, Smith SD. 1987. Ca^{2+}-45 cyclotron resonance in human lymphocytes. J Bioelect 6:13–22.

Lowe G, Meister M, Berg HC. 1987. Rapid rotation of flagellar bundels in swiming bacteria. Nature 325:637–640.

McLeod BR, Smith SD, Liboff AR. 1987. Calcium and potassium cyclotron resonance curves and harmonics in diatoms. J Bioelect 6:153–168.

Miller JA, Serio GF, Howard RA, Bear JL, Evans JE, Kimball AP. 1979. Subunit localizations of zinc(II) in DNA-dependent RNA polymerase from *Escherichia coli B*. Biochim Biophys Acta 579:291–297.

Moggia E, Chiabrera A, Bianco B. 1997. A Fokker–Plank analysis of the Langevin–Lorentz equation: application to ligand-receptor binding under electromagnetic exposure. J Appl Phys 82:4669–4677.

Noji H, Yasuda R, Yoshida M, Kinosita Jr K. 1997. Direct observation of the rotation of F1-ATPase. Nature 386: 299–302.

Panth H, Brenner MC, Wu FY. 1991. 1H NMR study of the interaction of ATP with *Escherichia coli* RNA polymerase containing in vivo-incorporated Co(II). Arch Biochem Biophys 291:307–310.

Pountney DL, Tiwari RP, Egan JB. 1997. Meta- and DNA-binding properties and mutational analysis of the transcription activating factor, B, of coliphage 186: a prokaryotic C4 zinc-finger protein. Protein Sci 6:892–902.

Prato FS, Carson JJL, Ossenkopp KP, Kavaliers M. 1995. Possible mechanism by which extremely low-frequency magnetic fields affect opioid function. FASEB J 9:807–814.

Rainteau D, Wolf C, Lavialle F. 1989. Effects of calcium and calcium analogs on calmodulin: a Fourier transform infrared and election spin resonance investigation. Biochim Biophys Acta 1011:81–87.

Satyshur KA, Rao ST, Pyzalska D, Drendel W, Greaser M, Sundaralingam M. 1988. Refined structure of chicken skeletal muscle troponin C in the two-calcium state at 2 Å resolution. J Biol Chem 263:1628–1647.

Stivers JT, Harris TK, Mildvan AS. 1997. Vaccinia DNA topoisomerase I: evidence supporting a free rotation mechanism for DNA supercoil relaxation. Biochemistry 36:5212–5222.

Suh WC, Leirmo S, Record Jr MT. 1992. Roles of Mg^{2+} in the mechanism of formation and dissociation of open complexes between *Escherichia coli* RNA polymerase and the lambda PR promoter: kinetic evidence for a second open complex requiring Mg^{2+}. Biochemistry 31: 7815–7825.

Zaychikov E, Martin E, Denissova L, Kozlov M, Markovtsov M, Kashlev M, Heumann H, Nikiforov V, Goldfarb A, Mustaev A. 1996. Mapping of catalytic residues in the RNA polymerase active center. Science 273:107–109.